Cellular Physiology and Biochemistry

Cell Physiol Biochem 2018;45:639-655
DOI: 10.1159/000487120
Published online: February 02, 2018
Accepted: November 01, 2017

Original Paper

The CFTR-Associated Ligand Arrests the Trafficking of the Mutant ΔF508 CFTR Channel in the ER Contributing to Cystic Fibrosis

Emily Bergbower[a,b,c] Clement Boinot[b,c] Inna Sabirzhanova[b,c] William Guggino[b,c] Liudmila Cebotaru[b,c]

[a]The Graduate Training Program in Cellular and Molecular Medicine, Johns Hopkins University School of Medicine, [b]Department of Physiology, Johns Hopkins University School of Medicine, [c]Department of Gastroenterology, Johns Hopkins University School of Medicine, Baltimore, MD, USA

Key Words
Trafficking • F508-del CFTR • Endoplasmic reticulum • PDZ-domain • Maturation

Abstract
Background/Aims: The CFTR-Associated Ligand (CAL), a PDZ domain containing protein with two coiled-coil domains, reduces cell surface WT CFTR through degradation in the lysosome by a well-characterized mechanism. However, CAL's regulatory effect on ΔF508 CFTR has remained almost entirely uninvestigated. ***Methods:*** In this study, we describe a previously unknown pathway for CAL by which it regulates the membrane expression of ΔF508 CFTR through arrest of ΔF508 CFTR trafficking in the endoplasmic reticulum (ER) using a combination of cell biology, biochemistry and electrophysiology. ***Results:*** We demonstrate that CAL is an ER localized protein that binds to ΔF508 CFTR and is degraded in the 26S proteasome. When CAL is inhibited, ΔF508 CFTR retention in the ER decreases and cell surface expression of mature functional ΔF508 CFTR is observed alongside of enhanced expression of plasma membrane scaffolding protein NHERF1. Chaperone proteins regulate this novel process, and ΔF508 CFTR binding to HSP40, HSP90, HSP70, VCP, and Aha1 changes to improve ΔF508 CFTR cell surface trafficking. ***Conclusion:*** Our results reveal a pathway in which CAL regulates the cell surface availability and intracellular retention of ΔF508 CFTR.

Introduction

Cystic Fibrosis (CF) is a common lethal autosomal recessive disorder caused by mutations in the Cystic Fibrosis Transmembrane Conductance Regulator (CFTR) gene [1, 2]). This gene encodes a cAMP-regulated chloride channel that is present on the apical membrane

W.B. Guggino and L. Cebotaru contributed equally to this work.

Liudmila Cebotaru
Johns Hopkins University School of Medicine
Hunterian 415, 725 North Wolfe Street, Baltimore MD (U.S.A.)
E-Mail lcebotaru@jhmi.edu

of epithelial cells lining the organs of the lungs, liver, pancreas, sweat ducts, intestines, and reproductive systems. Mutations in CFTR impair the salt and water balance of these tissues leading to host of clinical problems brought about by dehydrated secretions, and the buildup of thick mucus [3, 4]. CF airways are vulnerable to infection and inflammation, pancreatic ducts and the intestines are obstructed, sweat chloride levels are high, and male infertility is common. As a membrane protein, CFTR belongs to the ATP-binding cassette transporter family. Its correct function is dependent upon proper synthesis, maturation, and trafficking from the ER and Golgi to the plasma membrane.

There are over 2000 mutations that cause CF [5]. The most common mutation among patients is ΔF508, and approximately 90% of the patient population are carriers [6]. ΔF508 CFTR is a misfolded protein that is recognized as such by the ER quality control system. The protein is polyubiquitilated, translocated to the cytosol, and prematurely degraded by the 26S proteasome [7, 8]. Thus, the majority of ΔF508 CFTR is eliminated by the cell and cannot mature or reach the cell surface. As therapies for ΔF508 are important for the health of CF patients, targeting this protein remains the greatest clinical and research problem within the field.

CAL, also known as PIST (PDZ domain protein interacting specifically with TC10), GOPC (Golgi-associated PDZ and coiled-coil motif containing), and FIG (fused in glioblastoma) is a PDZ domain containing protein with two coiled-coil domains that interacts with the C-terminus of CFTR [9, 10]. Our lab has previously shown that CAL associates with the Golgi apparatus and reduces cell surface WT CFTR through promotion of lysosomal degradation [9, 11]. The effect of CAL on WT CFTR can be affected through a variety of regulator proteins. TC10, a small rho GTPase, binds to CAL in the region of its coiled-coil domain and promotes trafficking of WT CFTR to the cell surface when it is activated and in a GTP-bound state [12]. In contrast, Syntaxin 6 (STX6), a soluble N-ethylmaleimide-sensitive factor-activating receptor protein (SNARE), binds to CAL forming a complex that recruits E3 ubiquitin ligase MARCH2 and promotes transport of WT CFTR to the lysosome for degradation [13, 14]. Additionally, the effects of CAL on WT CFTR can be reversed through the overexpression of Na^+/H^+ exchanger regulatory factor 1 (NHERF1), a protein that anchors CFTR to the cytoskeleton [9].

While CAL's interactions with WT CFTR are well characterized, very little is known about its ability to regulate ΔF508 CFTR. Given that changes in CAL have been shown to improve ΔF508 CFTR chloride current [15], we investigated the mechanism by which CAL can improve ΔF508 CFTR function and plasma membrane trafficking. In this article, we demonstrate that CAL plays a significant role in the early trafficking of ΔF508 CFTR, regulating availability of cell surface ΔF508 CFTR and influencing ER retention.

Materials and Methods

Reagents and Antibodies

MG-132 was obtained from Sigma Aldrich. The HA-CAL plasmid and the GFP-ΔF508 CFTR plasmid were made in the Guggino lab. The KDEL-td-tomato plasmid was a generous gift from Dr. Carolyn Machamer (Johns Hopkins University School of Medicine, Baltimore, MD). The following primary antibodies were used: mouse monoclonal anti-CFTR 217/596/769 (Laboratory of Jack Riordan, University of North Carolina, Chapel Hill); mouse monoclonal anti-CFTR M3A7 (Millipore); mouse monoclonal anti-GFP (Roche); HA-probe (sc-7392), VCP (sc-133125), HSP70 (sc-66048), HSP40 (sc-59554), NHERF1, and Ezrin (sc-58758) were purchased from Santa Cruz Biotechnology; rabbit monoclonal anti-PIST (Abcam); and mouse monoclonal anti-AHSA1 (Abnova). Secondary antibodies used for immunofluorescence were conjugated to Alexa 488 and Alexa 594 (Invitrogen). CAL specific siRNA was purchased from Qiagen (GOPC_9).

Cell Culture and Transfection

CFBE41o- cells (derived by Dieter Gruenert; a cell line from bronchial epithelial cells of a cystic fibrosis patient), also called parental cells, were cultured in minimal essential medium Eagle (MEM, Invitrogen)

with 10% fetal bovine serum (FBS, Invitrogen), penicillin/streptomycin (Invitrogen), and glutamine (Invitrogen). CFBE-ΔF508CFTR cells (CFBE41o- cells stably expressing ΔF508 CFTR) were cultured in MEM with 10% FBS, penicillin/streptomycin, glutamine, and puromycin. CFBE-WTCFTR cells (CFBE41o- cells stably expressing wildtype CFTR) were cultured in MEM with 10% FBS, penicillin/streptomycin, glutamine, and hygromycin B. African green monkey kidney cell line COS-7 was maintained in DMEM with 10% FBS, penicillin/streptomycin, and L-glutamine. All cell lines were stored in a humidified 37°C CO_2 incubator. For plasmid transfection, cells were transiently transfected using 4μg of plasmid DNA and lipofectamine 2000 (Invitrogen) according to the manufacturer's instruction, and incubated for 48 hours. For knockdown, cells were transfected with 20nM siRNA using Interferin (Polyplus Transfection) and incubated for 48 hours.

Co-immunoprecipitation and Western Blotting

Cells were washed twice with cold Dulbecco's phosphate buffered saline (DPBS, Invitrogen) and then resuspended in lysis buffer (150 mM Tris HCl pH 7.5, 50 mM NaCl, 1% Nonidet P-40) with Halt Protease Inhibitor Cocktail and EDTA Solution (Thermo Fisher) added. After 30 minutes rotating at 4°C, the lysates were cleared by centrifugation at 15, 000 g for 15 minutes. Pellets were discarded, and supernatants were collected for further experimental use. Protein A/G Plus-Agarose beads (Santa Cruz Biotechnology) were mixed with lysates, and primary antibodies, and rotated overnight at 4°C. Beads were then washed five times with lysis buffer and incubated in Laemmli sample buffer at 37°C for 20 minutes. Total lysates were denatured in Laemmli sample buffer at 37°C for 20 minutes. The protein concentration of each sample was measured and equal amounts of total proteins were loaded onto 10% HCl-Tris gels. Proteins were separated by SDS-PAGE and transferred to PVDF membranes (BioRad). After transfer, membranes were blocked with 5% milk in tris-buffered saline with .05% Tween (TBST) for 1 hour. The membranes were incubated with primary antibodies in 5% milk in TBST at 4°C overnight. Membranes were then washed 3 times in TBST and incubated with the appropriate horseradish peroxidase-conjugated secondary antibody in 5% milk in TBST for an hour. Following secondary incubation, membranes were washed 3 times and incubated with Super Signal West Dura Extended Duration Substrate (Thermo Fisher) for two minutes. Results were visualized using a Fujifilm LAS4000 developer.

Cell-surface Biotinylation

Cells were washed twice with cold DPBS containing 1 mM Ca^{2+} and 1 mM Mg^{2+}. Following the wash, cells were incubated with 0.5 mg/ml sulfo-NHS-SS-biotin (Thermo Scientific) in DPBS with Ca^{2+} and Mg^{2+} at 4°C for 30 minutes. Free sulfo-NHS-SS-biotin was then quenched by washing with cold 50 mM glycine in DPBS three times. Cells were subsequently washed twice with DPBS containing 1 mM Ca^{2+} and 1 mM Mg^{2+} and twice with cold DPBS. Following these washes, cells were lysed with lysis buffer, rotated for 30 minutes, and the lysates were centrifuged at 15, 000 g at 4°C for 15 minutes. The supernatants were incubated with NeutrAvidin UltraLink Resin (Thermo Scientific) at 4°C for 1 hour. The beads were washed four times with lysis buffer, and proteins were eluted with Laemmli sample buffer at 37°C for 20 minutes. Biotinylated protein samples were analyzed by western blotting as described above.

Immunofluorescence and Fluorescent Microscopy

Zeiss LSM 510 laser scanning system and 63x oil-immersion lens were used. Cells were seeded onto cover glasses and later transiently transfected with various plasmids, as well as a CAL specific siRNA for 48 hours. The following steps were done at room temperature: cells were fixed with 4% formaldehyde for 15 minutes. Subsequently, cells were permeabilized with 0.3% Triton X-100 in DPBS for 5-7 minutes and blocked with 3% bovine albumin serum (BSA) for 45 minutes. After blocking, cells were incubated with primary antibodies and then with secondary antibodies conjugated to Alexa488 or Alexa 594. Cells were incubated with a 1:1000 dilution of DAPI for 5 minutes and mounted using ProLong Gold Antifade (Invitrogen). Images were cropped, adjusted, and exported as TIFs using Imaris Imaging Software. Figs. for publishing were put together using Adobe Photoshop. For quantification of colocalization, Pearson's correlation coefficients were calculated using Imaris Imaging Software.

Short Circuit Current Assay

Short-circuit current (I_{SC}) measurements were performed in a six-channel Easy-Mount chamber system (Physiologic Instruments, San Diego, CA) that accepts Snapwell filters (Corning Costar, Acton, MA; 3407). I_{SC}

was measured with a VCCMC6 multichannel voltage-current clamp amplifier (Physiologic Instruments) in the voltage-clamp mode. Data were acquired on an 1.71-GHz PC running Windows XP (Microsoft, Redmond, WA) and equipped with DI-720 (DATAQ Instruments, Akron, OH), with Acquire and Analyze version 2.3.159 (Physiologic Instruments) software. Cells were cultured to confluence on Snapwell filters before measurement. The cell monolayers were bathed on both sides with solution containing 115 mM NaCl, 25 mM sodium gluconate, 5 mM potassium gluconate, 1.2 mM $MgCl_2$, 1.2 mM $CaCl_2$, 10 mM D-glucose and 10 mM HEPES (pH 7.4 with NaOH). The mucosal side was replaced with a low Cl^- solution containing 139 mM sodium gluconate, 1.2 mM NaCl, 5 mM potassium gluconate, 1.2 mM $MgCl_2$, 1.2 mM $CaCl_2$, 10 mM D-glucose, and 10 mM HEPES (pH 7.4 with NaOH). The solution was constantly circulated, maintained at 37°C, and bubbled gently with air. Amiloride (20 μM) was added to the mucosal solution, and after stabilization, forskolin (10 μM) was added to the serosal chamber, followed by the CFTR channel inhibitor CFTRinh-172 (5 μM). The short circuit current is measured with a basolateral to apical chloride gradient to enhance the Cl^- transport out of the cells across the apical membrane to measure CFTR-dependent current more accurately.

Statistical Analysis

Data are displayed in bar graphs using Graphpad software. All quantitative results are given as means ± standard error (SE) which are represented by lines extending from each bar. Means and SEs are calculated from at least three independent experiments. Values of $p<0.05$ were considered significant.

Results

CAL Regulates ΔF508 CFTR Levels in Total Lysate of ΔF508-CFBE cells

Changes in intracellular levels of ΔF508 CFTR can be quantified through measurement of the CFTR B band and C band seen on western blots. The B band, which is approximately 150 kDa in size, represents the immature core-glycosylated form of ΔF508 CFTR. The C band, which is 170 kDa, represents the mature complex glycosylated form of ΔF508 CFTR [16]. A previous study reported that CAL knockdown enhanced ΔF508 CFTR maturation and chloride currents. The effect of CAL silencing was shown to be specific for ΔF508-CFTR and did not affect the expression of BCRP, another ABC transporter encoded by the *abcg2* gene or the α-subunit of Na/K ATPase [15]. We extended these observations by analyzing changes in the B band and C band of ΔF508 CFTR when CAL is inhibited in ΔF508-CFBE cells.

ΔF508-CFBE cells were transiently transfected with CAL specific siRNA and collected lysates were analyzed by western blot. The results of the western blot in Fig, 1A and summarized in Fig. 1 B-D confirm that after transfection with CAL specific siRNA, the expression of CAL protein is successfully reduced while ΔF508 CFTR B band and C band increase in the total lysate Fig. (1A-D). A negative scrambled control and a lipofectamine mock transfection control were also tested and shown to have no effect on expression levels of ΔF508 CFTR (Fig. 1F-G).

Results were then quantified for statistical analysis. After CAL knockdown, the immature B band of ΔF508 CFTR increases about 6 times compared to the control (Fig. 1B). The mature C band ΔF508 CFTR increases similarly compared to the control (Fig. 1C). These results were shown to be statistically significant (Fig. 1B, C). On the other hand, the ratio of B or C bands to the total CFTR did not change indicating that both changed in the same proportion (1D) CAL knockdown by siRNA was determined to be sufficient and effective via quantification, with percentage of median knockdown being 76% (Fig. 1E). Our data confirm that CAL knockdown in ΔF508-CFBE cells increases the immature B band and mature C band of ΔF508 CFTR to statistically significant levels (Fig.1).

CAL Binds to ΔF508 CFTR at the ER and is Degraded in the Proteasome

Since our data indicate that CAL can regulate levels of ΔF508 CFTR in total lysate, we next examined if CAL knockdown directly or indirectly affected ΔF508 CFTR trafficking through analysis of the binding relationship between the two proteins. A previous study has

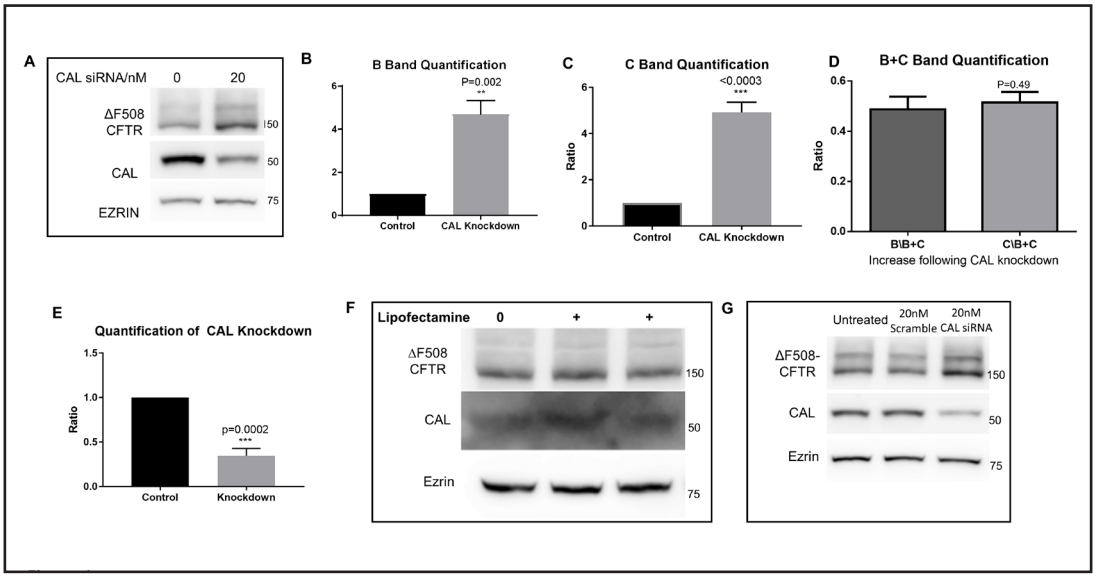

Fig. 1. CAL knockdown increases intracellular levels of the immature and mature forms of ΔF508 CFTR. (1A) ΔF508-CFBE cells were transfected with 20nM of CAL specific siRNA for 48 hours. Lysates were collected and run on western blots to assess the efficacy of the siRNA. CAL knockdown is clearly visible and ezrin is used as a loading control. (1B) Changes in immature ΔF508 CFTR (B band) were quantified in bar graph form from western blots 6 individual experiments. The increase in B band was determined to be statistically significant by two-sided one sample t-test compared to 1. Error bars, SE. (1C) Changes in mature ΔF508 CFTR (C band) were quantified in bar graph form from western blots of 6 individual experiments. The increase in C band was determined to be statistically significant by student's t-test Error bars, SE. Ratios for (B) and (C) were normalized to control by dividing each of the control band densities measured in the presence of normal levels of CAL and the CAL knockdown densities by the control band intensities (1D) Changes in the ratio of the B/B+C and the C/B+C ratios following CAL knockdown. The data were calculated from (B&C). One can see that knocking down CAL increased both mature and immature bands of CFTR but their respective ratio to the total quantity of CFTR remained unchanged. (1E) CAL was quantified by western blot, to assess median percent knockdown. Results are presented as a bar graph and median knockdown is 76% which was deemed statistically significant by two-sided one sample t-test compared to 1. Error bars, SE. (n=6). **p<0.01; ***p<0.001. (1F-G) Lipofectamine treatment or transfection with a negative scramble siRNA have no effect on CAL or levels of ΔF508 CFTR in total lysate. (1F) ΔF508-CFBE cells were treated with transfection agent lipofectamine alone for 48 hours. Lysates were collected and run on western blots to assess the effect of lipofectamine on ΔF508 CFTR in total lysate. No effect can be seen. Ezrin is used as a loading control. (1G) ΔF508-CFBE cells were transfected with either 20nM of CAL specific siRNA or 20nM of All Stars Universal Negative Scramble siRNA from Qiagen for 48 hours. Lysates were collected and run on western blots to assess the efficacy of the negative scramble versus the CAL siRNA. The negative scramble has no effect of intracellular levels of ΔF508 CFTR. CAL knockdown is clearly visible in CAL siRNA transfected samples and ezrin is used as a loading control.

shown that CAL can bind to WT CFTR in order to regulate it's trafficking to the lysosome, as opposed to the plasma membrane [9]. Here, COS-7 cells were transiently transfected with various GFP-tagged CFTR plasmids or HA-CAL and collected total lysates were subjected to co-immunoprecipitation. Samples from total lysate and the binding fractions were then run on western blots for analysis.

In Fig. 2A, there are five lanes for assessment. Lane 1 is the untransfected control, and as such, no CFTR appears in the total lysate (top) or Co-IP fractions (bottom). Since CFTR is not present, CAL is not observed in the Co-IP fraction (bottom). Given that an anti-CAL antibody was used, there is some endogenous level of CAL in COS-7 cells so a faint band is observed in the total lysate (top). Lane 2 has been transfected with GFP-WTCFTR plasmid and pulled

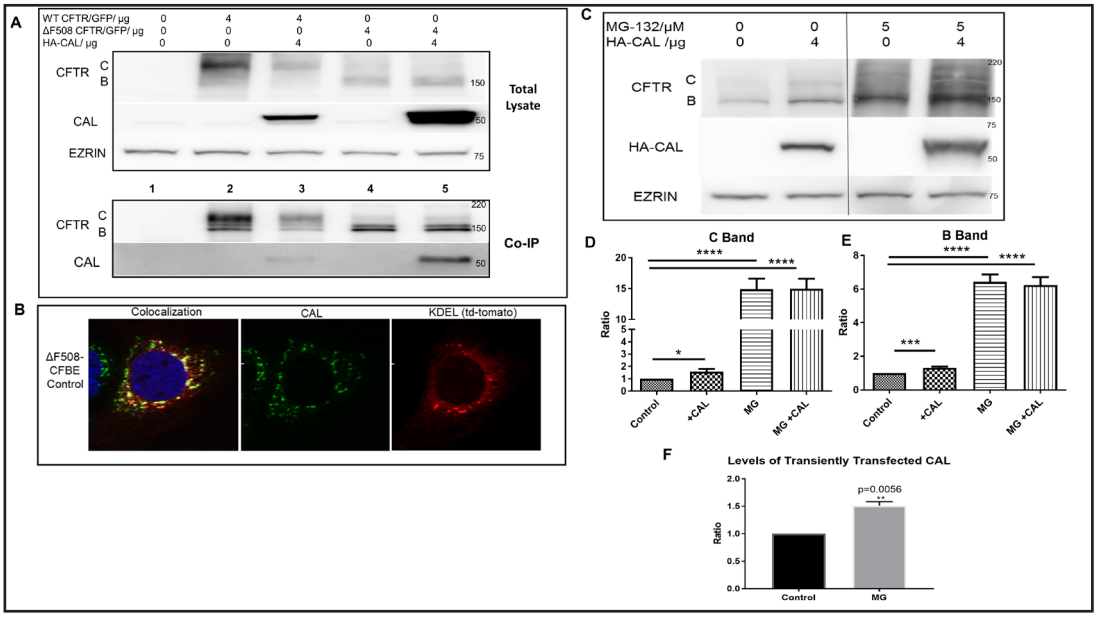

Fig. 2. CAL binds to ΔF508 CFTR, localizes to the ER, and is degraded by the 26S proteasome. (2A) COS-7 cells were either transfected with GFP-ΔF508CFTR, GFP-WTCFTR, and/or HA-CAL plasmids for 48 hours. Cell lysates were collected and used in co-immunoprecipitation experiments with A/G beads and GFP antibody (n=3). Samples were assessed via western blot and probed for GFP and HA to detect binding of tagged proteins. Binding of WT CFTR to HA-CAL (Lane 3) and binding of ΔF508 CFTR to HA-CAL (Lane 5) are detectable in the Co-IP fractions. Untransfected COS-7 cells were used as a negative control (Lane 1). Please note that although HA-CAL was transfected, CAL was detected using an anti-CAL antibody produced in the laboratory [11]. The small difference in molecular wt. between endogenous CAL and transfected CAL represents the addition of the HA tag. (2B) ΔF508-CFBE cells were plated on coverslips and transfected with KDEL td-tomato plasmid for 48 hours. Cells were fixed, and stained with 4',6-diamidino-2-phenylindole (DAPI; blue, nucleus) and antibodies against PIST (green, CAL). KDEL is detected by its tomato tag (red). Representative extended focus images are shown. (2C) ΔF508-CFBE cells were either transfected with HA-CAL plasmid or left untransfected for 48 hours. (2D-E) Quantification of C band and B band respectively. Data normalized to the control. (2F) Quantification of CAL, data normalized to control. Cells were treated with MG-132 for 12 hours. Lysates were collected and run on western blots (4 individual experiments). Westerns were probed for CFTR, CAL, and Ezrin (loading control). All images come from the same gel but some lanes have been cropped (denoted by a line marking the site of the crop) since it was a dose dependent experiment. CAL protein levels were quantified and the increase in CAL protein with MG-132 treatment was established to be statistically significant by two-sided one sample t-test compared to 1. Error Bars, SE. (n=3 independent experiments and quantification was performed on four cells from each slide. *p<0.05; **p<0.01; ****p<0.0001.

down with an anti-GFP antibody. Thus, WT-CFTR is observed in the total lysate (top) and Co-IP fractions (bottom) as detected by an anti-GFP antibody. Levels of endogenous CAL are so low that no binding is visible.

Lane 3 has been co-transfected with GFP-WTCFTR and HA-CAL. Enhancing intracellular levels of CAL through transfection results in a visible band for CAL in the Co-IP fraction indicating that WT CFTR and HA-CAL are bound. Lane 4 has been transfected with GFP-ΔF508CFTR plasmid. Thus, ΔF508 CFTR is observed in the total lysate (top) and Co-IP fractions (bottom) but no binding to CAL is visible. Finally, lane 5 has been co-transfected with GFP-ΔF508CFTR and HA-CAL. Here, binding of ΔF508 CFTR and CAL is visible in the Co-IP fraction (bottom). These results indicate that not only does CAL bind to wt-CFTR as was shown previously [9] but also to ΔF508 CFTR (Fig. 2A).

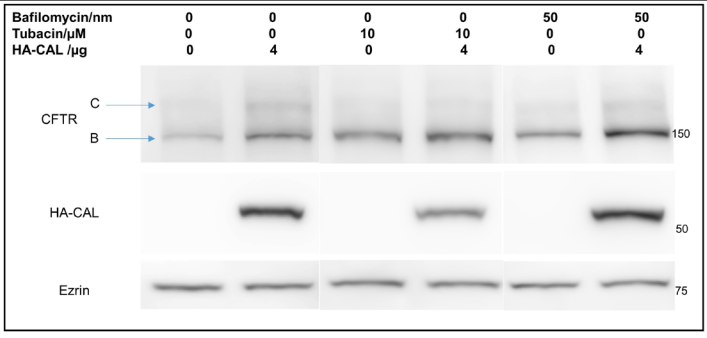

P values	Bafilomycin A	Bafilomycin A +HA-CAL	Tubacin	Tubacin +HA-CAL
B Band	0.9997	0.9952	0.6988	0.6658
C Band	0.9919	0.9965	0.7024	0.9318

Fig. 3. Treatment with bafilomycin and tubacin does not have a significant effect on ΔF508 CFTR levels in total lysate. ΔF508-CFBE cells were either transfected with HA-CAL plasmid or left untransfected for 48 hours. Cells were treated with Tubacin or Bafilomycin for 12 hours. Lysates were collected and run on western blots (4 individual experiments). Westerns were probed for CFTR, CAL, and Ezrin (loading control). All images come from the same gel but some lanes have been cropped. Comparisons to control lane 1 were made with ordinary one-ANOVA using Dunnett's multiple comparison test (n=3).

To establish the cell compartment in which CAL binds ΔF508 CFTR in ΔF508-CFBE cells, a series of co-immunofluorescence experiments were performed (Fig. 2B). ΔF508-CFBE cells were transfected with KDEL-td-tomato plasmid (a gift from Dr. Carolyn Machamer) and examined by fluorescence microscopy. CAL is shown to colocalize with KDEL, indicating that CAL localizes at the ER (Fig. 2B). These results suggest that some CAL interacts with ΔF508 CFTR at the level of the ER.

Next, to establish the site of CAL degradation in ΔF508-CFBE cells, we investigated various organelles linked to protein degradation. Previous studies focused on WT CFTR tightly couple CAL degradation to the lysosome, as it directs WT CFTR there for degradation [9, 11]. In Fig. 2C, ΔF508-CFBE cells were transfected with HA-tagged CAL and treated with MG-132, an inhibitor of the 26S proteasome. MG-132 visibly increased the B band and C band of ΔF508 CFTR to as similar amount in CAL transfected and untransfected cells (Fig. 2D & E). Treatment with MG-132 increased levels of CAL to 1.5 times that of the control, indicating that CAL is degraded in the 26S proteasome (Fig. 2F). Following treatment with bafilomycin and tubacin, no changes in CAL were observed (Fig. 3). This result indicates that CAL degradation is not lysosomal or aggresomal in ΔF508-CFBE cells.

CAL Knockdown Generates Cell Surface Expression of Mature ΔF508 CFTR

Since surface expression of mature CFTR is key to correction of the mutant protein, we sought to determine if CAL knockdown could produce mature cell surface expressed ΔF508 CFTR. It is thought that very little ΔF508 CFTR reaches the cell surface, as most of it is prematurely degraded in the proteasome. However, a small fraction of ΔF508 CFTR is able to exit the ER and escape the ER-associated degradation (ERAD) pathway but is not stable at the cell periphery [17]. To determine if CAL knockdown affects ΔF508 CFTR surface expression, we preformed several cell surface biotinylation.

In Fig. 4A, mature cell surface C band was observed in the biotinylation fraction of the WT sample (top panel; Lane 1). Additionally, a very faint band representing immature cell surface B band was observed in the untransfected control ΔF508-CFBE sample (top panel; Lane 2).

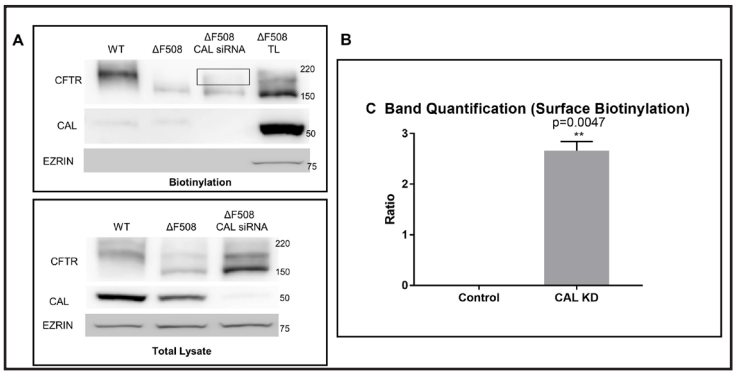

Fig. 4. CAL knockdown creates mature cell surface ΔF508 CFTR. (4A) ΔF508-CFBE cells were transfected with 20nM CAL specific siRNA for 48 hours. Lysates were collected from control and siRNA treated cells, and used in biotinylation assays to assess cell surface expression of the ΔF508 CFTR. Samples from the biotinylated fractions and the total lysate fractions were run on western blots (4 individual experiments). Western blots were probed for CFTR, CAL, and Ezrin. Ezrin is both a loading control for total lysate (bottom) and a control for the biotinylation (top) since ezrin is not expressed at the plasma membrane and as such is completely absent from all biotinylated samples. (4B) C band from the siRNA transfected ΔF508-CFBE biotinylated samples. A small amount of CAL in the biotinylated fractions most likely represents binding to CFTR during the streptavidin pull-down. (Top: lane 3) were quantified from 4 individual experiments and compared against the null for statistical significance by two-sided one sample t-test compared to 0. The result is significant with **p>0.01. Error bars, SE.

Most importantly, Fig. 4A shows that in CAL siRNA transfected ΔF508-CFBE cells, both mature C band and immature B band are present on the cell surface (top panel; Lane 3, black box). The *de novo* C band was quantified, compared to the null, and found to be statistically significant (Fig. 4B). This result is critical, as it shows that the CAL protein is integral to regulating the cell surface expression of ΔF508 CFTR, since knockdown of CAL led to the *de novo* production of cell surface C band. The presence of B band on the surface when CAL is inhibited indicates that some fraction of the intracellular immature ΔF508 CFTR can traffic to the surface when freed from CAL binding at the ER. We have also observed previously (see [12] Fig. 1A) that even with wt-CFTR a small leakage of B band to the cell surface occurs particularly when processing of wt-CFTR is enhanced by activation of TC10. One suggestion is that core glycosylated, B band, form of ΔF508-CFTR traffics via a PDZ domain interaction with GRASP, a Golgi reassembly stacking protein [18]. During periods of ER stress, CFTR binds to GRASP increasing the trafficking of the B band to the plasma membrane. Perhaps in the absence of CAL, GRASP can more readily bind to CFTR. Although a possibility, precisely how the immature B band reaches the plasma membrane in our experimental circumstances will require further investigation.

CAL Knockdown Averts Arrest of ΔF508 CFTR in the ER

To determine how knockdown of CAL can affect the progression of ΔF508 CFTR trafficking, we set out to assess colocalization of ΔF508 CFTR with the ER, Golgi, and plasma membrane. Prior studies have already established the localization of WT CFTR and CAL relative to cellular organelles [9, 11]. Control experiments show that CAL and CFTR colocalize in ΔF508-CFBE cells (Fig. 5A), while CAL knockdown results in decreased colocalization between CAL and ΔF508 CFTR as expected. Additionally, CAL knockdown is shown to affect the distribution of ΔF508 CFTR in the cell, resulting in greater spread throughout the cell and less concentration around the ER (Fig. 5A). We then used Imaris Imaging Software to calculate Pearson's correlation coefficients to determine the quantitative colocalization of ΔF508 CFTR and CAL when CAL is inhibited compared to controls. When CAL is inhibited by siRNA, Pearson's correlation coefficients decrease significantly (Fig. 5B).

When ΔF508 CFTR colocalization with KDEL was assessed, we observed a high level of colocalization between the two proteins (Fig. 5C). After transfection with CAL siRNA, colocalization of ΔF508 CFTR with KDEL decreased and improved the distribution of ΔF508 CFTR throughout the cell (Fig. 5C). These results demonstrate that CAL knockdown affects

ΔF508 CFTR distribution and results in the release of ΔF508 CFTR from the ER, enhancing its trafficking to the cell surface. We then used Imaris to calculate Pearson's correlation coefficients to determine the quantitative colocalization of ΔF508 CFTR and KDEL when CAL is inhibited compared to controls. When CAL is inhibited by siRNA, Pearson's correlation coefficients decrease significantly (Fig. 5D).

We subsequently sought to establish if CAL knockdown would improve ΔF508 CFTR maturation and cell surface expression by observing how much ΔF508 CFTR colocalizes with markers for the Golgi and plasma membrane. Data from untransfected control ΔF508-CFBE cells shows that very little ΔF508 CFTR colocalizes with the Golgi (Fig. 6A). This is consistent with other studies. However, after CAL knockdown, we observed that the level of colocalization between the Golgi and ΔF508 CFTR increased (Fig. 6A).We calculated Pearson's correlation coefficients to determine the quantitative colocalization of ΔF508 CFTR and Golgin-97 when CAL is inhibited and noted a corresponding statistically significant increase in the coefficient (Fig. 6B).

As for plasma membrane colocalization, data from untransfected control ΔF508-CFBE cells shows that no ΔF508 CFTR reaches the plasma membrane (Fig. 6C). This is consistent

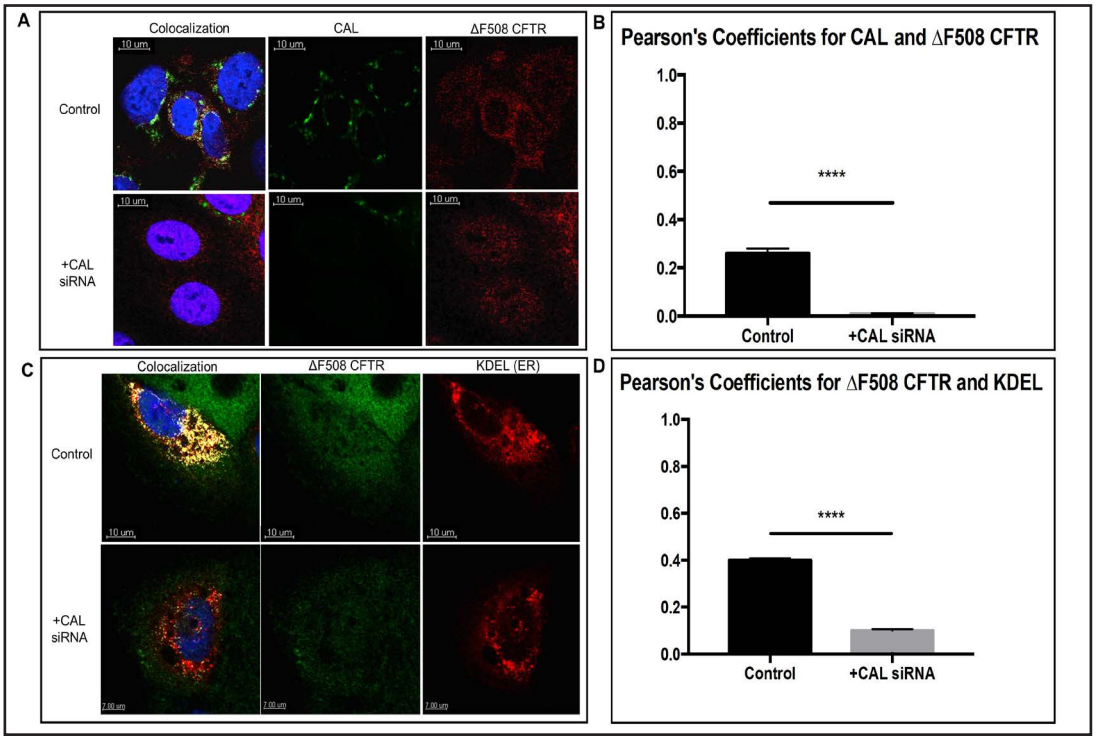

Fig. 5. CAL changes ΔF508 CFTR intracellular distribution and arrests its trafficking in the ER. (5A) ΔF508-CFBE cells were plated on coverslips and transfected with 20nM of CAL specific siRNA for 48 hours. Cells were then fixed and stained with DAPI (blue, nucleus) and antibodies against PIST (green, CAL) and CFTR 769 (red, ΔF508-CFTR). CFTR antibody 769 targets NBD2 (aa 1204-1211). Representative extended focus images are shown. (5B) The graph shows Pearson's correlation coefficients of ΔF508-CFTR and CAL when CAL is inhibited compared to control samples. The coefficients were calculated using Imaris Imaging Software. Pearson's correlation coefficients were reduced by CAL knockdown. Results are means ±SE. (n=5) ****p<0.0001. (5C) ΔF508-CFBE cells were plated on coverslips and transfected with 20nM of CAL specific siRNA for 48 hours. Cells were also transfected with KDEL td-tomato plasmid (red, ER). Cells were fixed and stained with DAPI (blue, nucleus) and antibodies against CFTR 769 (green, ΔF508 CFTR). Representative extended focus images are shown. (5D) The graph shows Pearson's correlation coefficients of ΔF508-CFTR and KDEL when CAL is inhibited compared to control samples. The coefficients were calculated using Imaris Imaging Software. Pearson's correlation coefficients were reduced by CAL knockdown. Results are means ±SE. (n=5) ****p<0.0001 using a two-sided two sample "t" test. N=number of independent experiments.

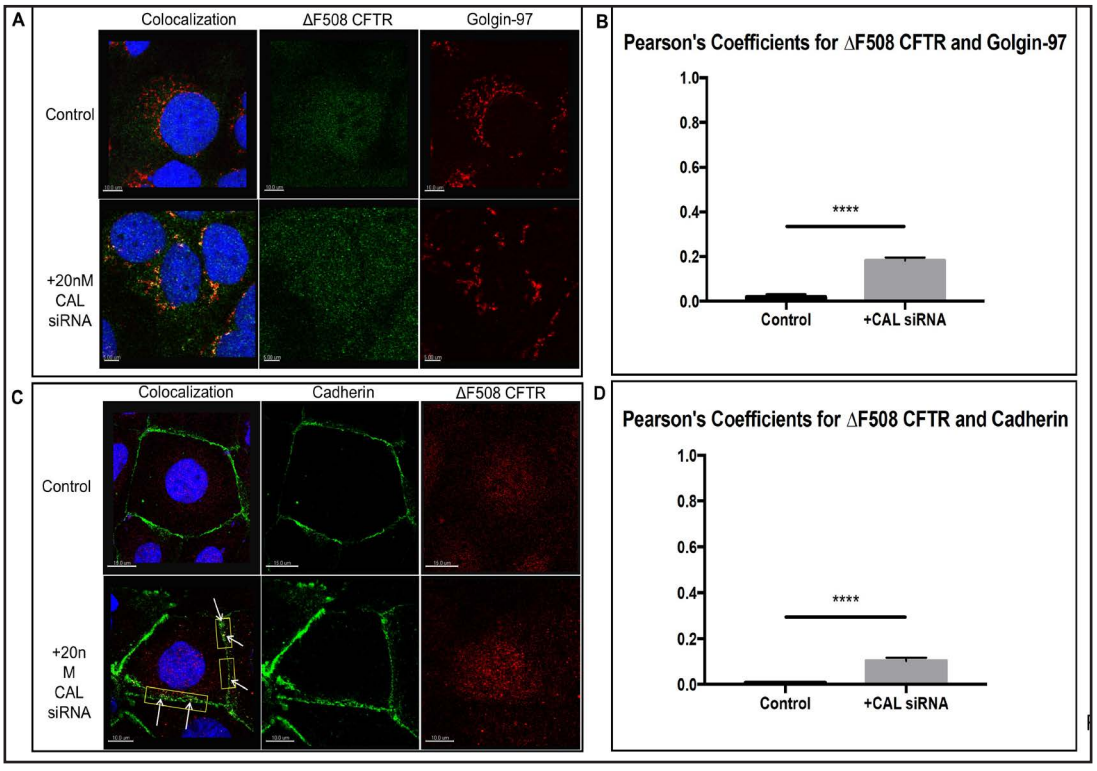

Fig. 6. CAL inhibition causes ΔF508 CFTR trafficking to the plasma membrane through the Golgi apparatus. (6A) ΔF508-CFBE cells were plated on coverslips and transfected with 20nM of CAL specific siRNA for 48 hours. Cells were fixed and stained with DAPI (blue, nucleus) and antibodies against Golgin-97 (red, Golgi) and CFTR 769 (green, ΔF508 CFTR). CFTR antibody 769 targets NBD2 (aa 1204-1211). Representative extended focus images are shown. (6B) The graph shows Pearson's correlation coefficients of ΔF508-CFTR and Golgin-97 when CAL is inhibited compared to control samples. The coefficients were calculated using Imaris Imaging Software. Pearson's correlation coefficients were increased with CAL knockdown. Results are means ±SE. (n=5) ****p<0.0001. (6C) ΔF508-CFBE cells were plated on coverslips and transfected with 20nM of CAL specific siRNA for 48 hours. Cells were fixed and stained with DAPI (blue, nucleus) and antibodies against pan-cadherin (green, plasma membrane) and CFTR 769 (red, ΔF508 CFTR). Areas of colocalization give off a yellow signal (yellow boxes, white arrows). Representative extended focus images are shown. (6D) The graph shows Pearson's correlation coefficients of ΔF508-CFTR and cadherin when CAL is inhibited compared to control samples. The coefficients were calculated using Imaris Imaging Software. Pearson's correlation coefficients were increased with CAL knockdown. Results are means ±SE. (n=5) ****p<0.0001 using a two-sided two sample "t" test. N=number of independent experiments.

with the rest of the data presented in this article. Interestingly, after CAL knockdown, colocalization between plasma membrane marker cadherin and ΔF508 CFTR is observed (Fig. 6C; yellow boxes with white arrows). When Pearson's correlation coefficients were calculated, we observed a significant increase in quantitative colocalization between ΔF508 CFTR and cadherin (Fig. 6D).

Chaperone Proteins are Critical for Regulating ΔF508 CFTR Trafficking Pathways

Chaperone proteins are integral to proper cellular function and viability due to the various roles they play within the cell. One of the most well characterized functions of chaperones is their ability to fold and transport other immature intracellular proteins. Without chaperones, plasma membrane expressed proteins such as CFTR would not reach the cell surface.

In order to elucidate the mechanism by which CAL knockdown causes the production of mature cell surface ΔF508 CFTR, we selected a set of chaperone proteins for assessment that

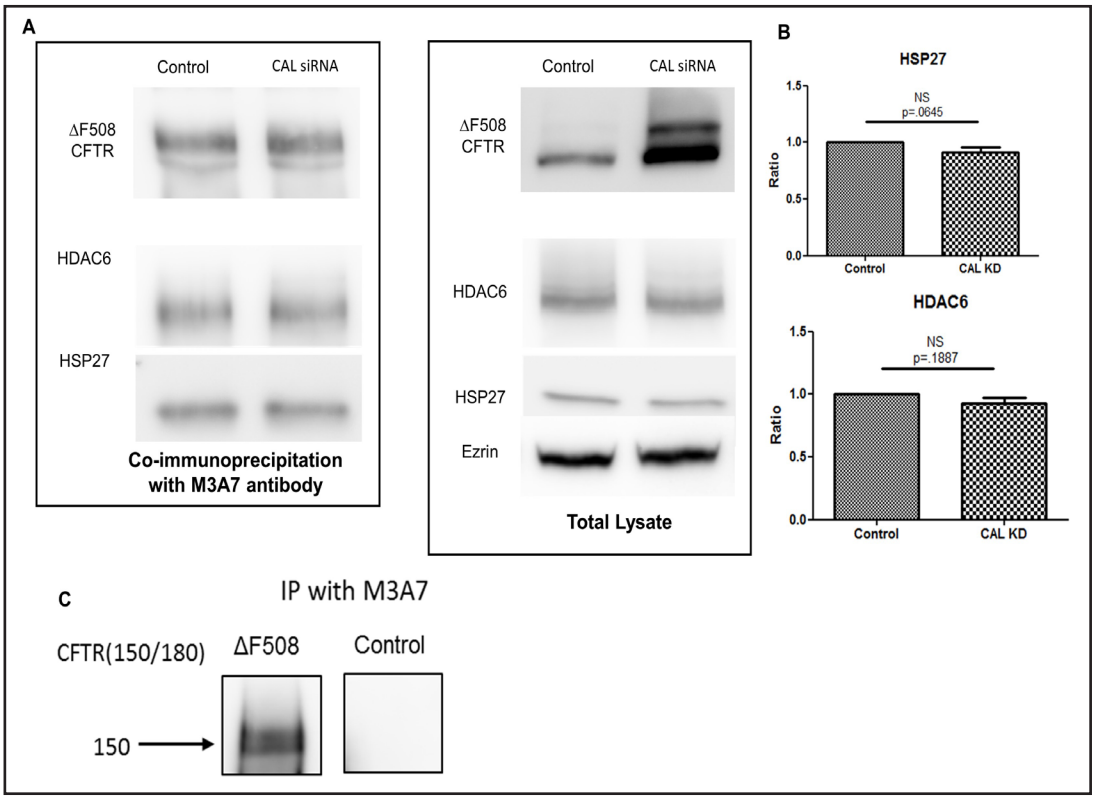

Fig. 7. HDAC6 and HSP27 binding to ΔF508 CFTR is unaffected by CAL knockdown. (7A) ΔF508-CFBE cells were transfected with CAL specific siRNA for 48 hours. Lysates were collected and used in co-immunoprecipitation experiments with A/G beads and CFTR specific antibody M3A7 (to pulldown ΔF508 CFTR). Samples from the co-immunoprecipitation fraction (left panel) and from the total lysate fraction (right panel) were assessed by western blot. (7B) (5 individual experiments, p value was not significant). Membranes were probed with antibodies against CFTR, HDAC6, HSP27, and Ezrin (loading control). CAL knockdown for this experiment is shown in total lysate of Fig. 8B of this paper. (7C) Control experiment was performed where an immunoprecipitation was performed with (left panel) CFTR or without (right panel) CFTR antibodies. Please note that there are no bands in the control lane indicating that protein does not bind non-specifically to the beads. Methods: 2000 mg protein was used for IP. Samples and lysis buffer (with Halt protease inhibitor) totaled 1 mL with 7uL M3A7 and 120uL beads: for control, sample with lysis buffer 1 mL with 120uL beads but no antibody. The two experiments were taken from the same blot.

are known to interact with both WT CFTR and ΔF508 CFTR. Chaperone proteins of interest included the following: HSP27, HSP40, HSP70, HSP90, HDAC6, HDAC7, VCP, and Aha1. In the experiments that followed, ΔF508-CFBE cells were transfected with CAL siRNA and cell lysates were collected for co-immunoprecipitation analysis (see Fig. 7 for the negative control).

No changes in binding were observed for HSP27, and HDAC6 (Fig. 7A-C). However, when CAL is inhibited by siRNA, small but no significant changes were observed in ΔF508 CFTR binding to HSP40, Aha1, and HSP70 (Fig. 8A & B). Importantly the binding to HSP90 increased and to VCP decreased (Fig. 8A). These results were statistically significant (Fig. 8B). Our data reveals that cell surface expression of ΔF508 CFTR due to CAL knockdown is driven by increases in pro-folding chaperones such as HSP90 and decreases in anti-folding chaperones such as VCP. However, changes in HSP40 are neither pro nor anti-folding but correlate to partner protein HSP70. These results confirm that CAL knockdown improves ER to Golgi trafficking and subsequent protein maturation through enhanced binding to profolding chaperones.

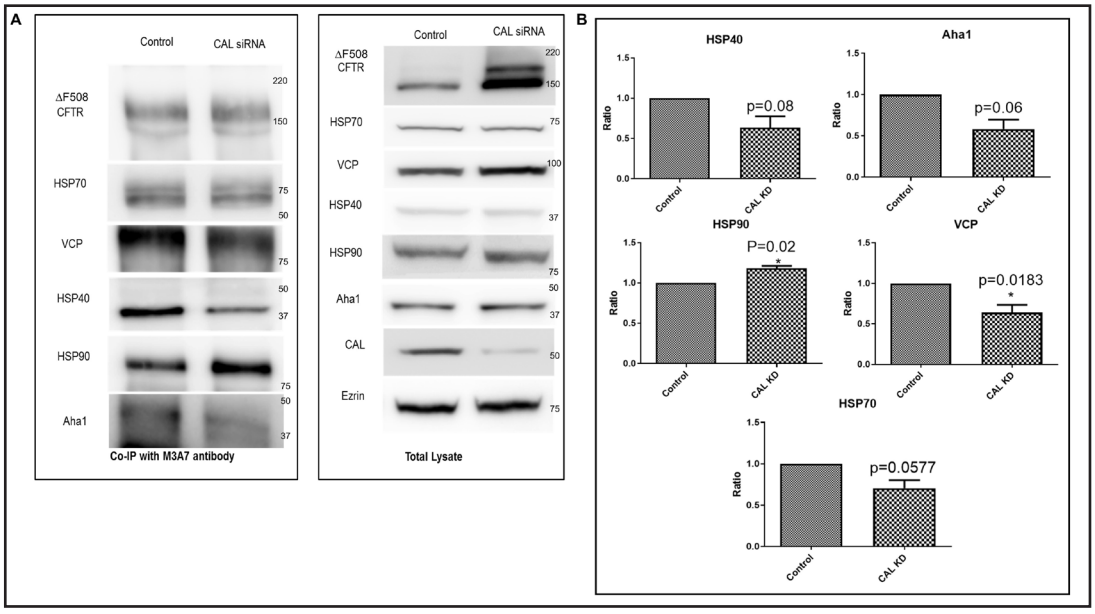

Fig. 8. CAL inhibition changes ΔF508 CFTR binding to chaperone proteins in order to improve ΔF508 CFTR cell surface trafficking. (8A) ΔF508-CFBE cells were transfected with CAL specific siRNA for 48 hours. Lysates were collected and used in co-immunoprecipitation experiments with A/G beads and CFTR specific antibody M3A7 (to pulldown ΔF508 CFTR). Samples from the co-immunoprecipitation fraction (left panel) and from the total lysate fraction (right panel) were assessed by western blot (5 individual experiments). Membranes were probed with antibodies against CFTR, HSP90, VCP, HSP40, HSP90, Aha1, CAL, and Ezrin (loading control). CAL knockdown is visible in total lysate. (8B) Changes in ΔF508 CFTR binding to HSP40, HSP90, HSP70, VCP, and Aha1 were quantified in bar graph form from western blots of replicate experiments. Error bars, SE. Data were analyzed by a two-sided one sample t-test compared to 1. *p<0.05.

Changes in NHERF1 were also measured under conditions of CAL knockdown. NHERF1 is a scaffold protein that serves to anchor CFTR to the cytoskeleton through a complex of proteins [19]. We observed a statistically significant increase in NHERF1 in the total lysate of cells that had been transfected with CAL siRNA (Fig. 7). This data shows that plasma membrane scaffolding protein NHERF1 exists in greater quantity intracellularly when CAL is inhibited, reflecting the need to stabilize a population of mature ΔF508 CFTR at the plasma membrane.

Changes in NHERF1 were also measured under conditions of CAL knockdown. NHERF1 is a scaffold protein that serves to anchor CFTR to the cytoskeleton through a complex of proteins [19]. We observed a statistically significant increase in NHERF1 in the total lysate of cells that had been transfected with CAL siRNA (Fig. 9). This data shows that plasma membrane scaffolding protein NHERF1 exists in greater quantity intracellularly when CAL is inhibited, reflecting the need to stabilize a population of mature ΔF508 CFTR at the plasma membrane.

CAL Knockdown Creates Functional Cell Surface ΔF508 CFTR by Short Circuit Current

Since we were able to show that CAL knockdown by siRNA results in cell surface expression of mature ΔF508 CFTR, we wanted to know whether this mature ΔF508 CFTR was functional. To determine if CAL knockdown increased chloride current compared to control samples, we utilized the short circuit current assay (Fig. 10). During the experiment, cells were in the presence of 10uM forskolin, which is used to raise levels of cAMP. During data collection, 30uM of genistein was applied, which has been shown to increase ΔF508 CFTR activity via potentiation. When genistein is applied, a peak in chloride current can be observed (Fig. 10A). Finally, 10uM of CFTR specific inhibitor 172 is applied at the end of the

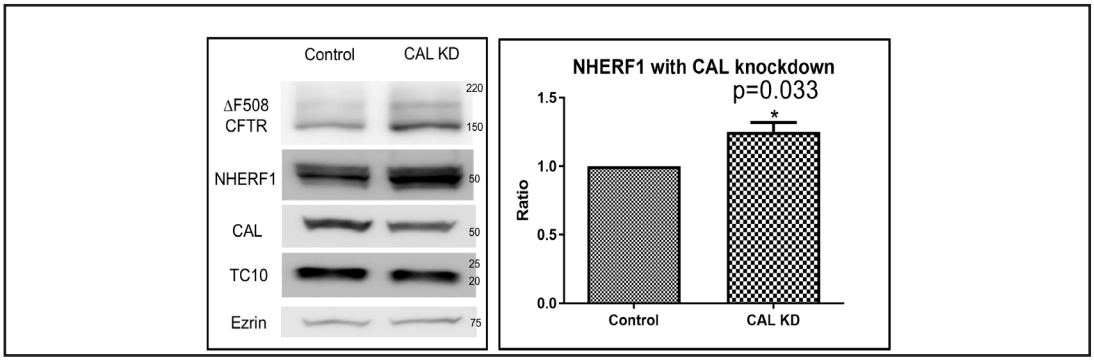

Fig. 9. NHERF1 acts as a scaffold for ΔF508 CFTR at the plasma membrane when CAL is inhibited. ΔF508-CFBE cells were transfected with 20nM of CAL specific siRNA for 48 hours. Lysates were collected and assessed by western blot. Membranes were probed for CFTR, NHERF1, CAL, TC10, and ezrin (loading control). Changes in NHERF1 protein levels were quantified in bar graph form from western blots of 3 individual experiments. The increase in NHERF1 protein when CAL is inhibited is statistically significant. Error Bars, SE. Changes in NHERF1 protein levels were quantified in bar graph form from western blots of replicate experiments. The decrease in NHERF1 protein when CAL is overexpressed is statistically significant by two-sided one sample t-test compared to 1; $p<0.05$. Error bars, SE.

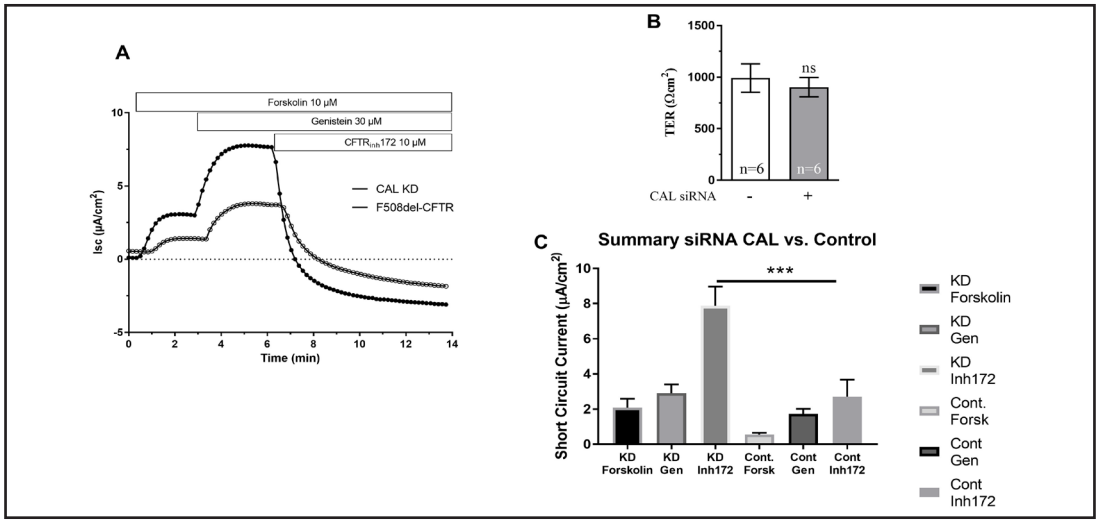

Fig. 10. CAL inhibition enhances ΔF508 CFTR chloride current by short circuit current. (10A) Cells were plated in snapwell filters and transfected with 20nM of CAL siRNA or for 48 hours. Measurements were performed in a six-channel Easy-Mount chamber system that accepts Snapwell filters. I_{SC} was measured with a VCCMC6 multichannel voltage-current clamp amplifier. Normalized Δ Isc and absolute magnitude of the transepithelial resistance (TER) is presented in bar graph form. Error bars, SE. (10B) This current amplitude graph (10C) displays the same data shown in (A). Note that cells were treated with forskolin, genistein and CFTR inh-172 and chloride current levels were recorded throughout. To accomplish these experiments we split a T75 flask among 6 wells to ensure that the Snapwell filters reach confluence within 4 days. Data analyzed using ANOVA with Tukey multiple comparisons test; ***$p<0.001$.

experiment as a control, to observe a decrease in chloride current for all samples (Fig. 10A). There is no change in transepithelial resistance (TER) associated with CAL silencing (Fig. 10B). Our results show that samples transfected with CAL specific siRNA have a statistically significant higher chloride current amplitude compared to the control samples (Fig. 10C). The data confirms that CAL knockdown leads to the production of mature ΔF508 CFTR that is functional at the cell surface.

Discussion

Our results suggest a pathway in which CAL can arrest plasma membrane trafficking of ΔF508 CFTR in the ER through binding. When the interaction between these two proteins is inhibited, cell surface expression of functional ΔF508 CFTR occurs through a Golgi-associated trafficking pathway. We have demonstrated that this pathway is regulated by chaperone and scaffold proteins that serve to either stabilize the arrested ER pool of ΔF508 CFTR or improve its cell surface trafficking. Finally, we have established that CAL, a traditionally trans-Golgi associated protein, localizes to the ER, binds to ΔF508 CFTR, and can be degraded in the proteasome which demonstrates that establishing it as a regulator of early ΔF508 CFTR trafficking and degradation is a reasonable conclusion.

It was previously demonstrated that CAL inhibition extends the half-life of ΔF508 CFTR and increases ΔF508 CFTR mediated chloride currents in polarized monolayers [15]. In this present study, we observed that inhibition of CAL by siRNA leads to an increase in the C band and B band of ΔF508 CFTR in the total lysate of ΔF508 CFBE cells. When we assessed cell surface expression of ΔF508 CFTR, we saw an increase in the mature cell surface C band of ΔF508 CFTR. Additionally, we showed that ΔF508 CFTR colocalizes with plasma membrane marker cadherin when CAL is inhibited in ΔF508 CFBE cells. This suggests that inhibition of CAL releases ΔF508 CFTR from being bound to CAL at the level of the ER and permits trafficking to the cell surface.

We postulate that this mature, C band of ΔF508 CFTR generated through CAL inhibition traffics to the plasma membrane via a pathway including the Golgi. This is supported by the fact that ΔF508 CFTR colocalization with the Golgi increases, and that ΔF508 CFTR has acquired complex Golgi-associated glycosylation. Additionally, we have also shown that the mature cell surface ΔF508 CFTR produced by CAL inhibition is functional. Results from short circuit current studies demonstrate that CAL inhibition increases ΔF508 CFTR mediated chloride currents to twice that of controls. We posit, due to these results, that CAL may be a useful clinical target among patients receiving combination therapy. These results are significant because currently there are no highly effective FDA-approved therapies for treating patients with the ΔF508 mutation. While combination therapy using Lumacaftor and Ivacaftor is FDA-approved and in use, the drug combination provides a modest level of clinical benefit to patients [20].

Several key chaperone proteins regulate the molecular mechanism of CAL inhibition promoting mature functional cell surface ΔF508 CFTR. Namely, VCP, HSP70, HSP40, Aha1, HSP90, and NHERF1. VCP is a Type II AAA ATPase that is a component of ER retrotranslocation machinery and is tied to the proteasomal degradation pathway [21, 22]. It was identified as a binding partner for ΔF508 CFTR in a proteomics screen [21]. It has also been shown that VCP and gp78, an autocrine motility factor, form complexes with CFTR targeted for proteasomal degradation [23]. Our study finds that VCP binding to ΔF508 CFTR in ΔF508-CFBE cells decreases when CAL is inhibited. Thus, our results reveal that inhibition of CAL leads to cell surface expression of mature functional ΔF508 CFTR most likely through suppression of the proteasomal degradation pathway. Less ΔF508 CFTR is bound to VCP, and thus even more is available to leave the ER, and traffic to the surface via the Golgi instead.

The stress-inducible HSP70 (HSPA1A) has an ATP-dependent mechanism and an important role in CFTR folding. DNAJ (HSP40) proteins are required for HSP70 to function in promoting or suppressing protein folding pathways. HSP70 links to HSP90 via HOP to complete chaperone assisted folding, but HSP70 also interacts with E3 ubiquitin ligase CHIP to drive premature protein degradation [24]. Additionally, it has been shown that overexpression of HSP70 and co-chaperone DNAJB1 induced only very modest improvements in trafficking and stabilization of ΔF508 CFTR [25, 26]. Our results show that binding of HSP70 and ΔF508 CFTR decreases to a small extent when CAL is inhibited, perhaps inhibiting the HSP70/CHIP anti-folding interaction in order to promote cell surface expression of ΔF508 CFTR. Nevertheless, the role of HSP70 in this trafficking pathway requires greater investigation.

Molecular chaperones HSP40, HSP90, and Aha1 assist in the productive folding of CFTR. Prior studies established that overexpression of HSP40 (Hdj-1) decreases the degradation rate of immature core-glycosylated WT CFTR [26]. However, the same study noted that ΔF508 CFTR degradation rates seemed unaffected by HSP40 overexpression [26]. This is consistent with our observation that the levels of CAL are not tightly linked to those of HSP40 in stabilizing ΔF508-CFTR.

Cell surface rescue of ΔF508 CFTR can be initiated by partial knockdown of HSP90 co-chaperone Aha1 [27]. Aha1 is a potent stimulator of HSP90 ATPase activity and acts as a late cofactor of the HSP90 complex [28, 29]. WT CFTR that is destined for the cell surface is exchanged from HSP40/HSP70 complexes to HSP90 cargo-specific complexes [29]. Reduced levels of Aha1 binding may very well improve the trafficking and maturation of ΔF508 CFTR by enhancing CFTR-Hsp90 interactions [27, 29] however, the binding of Aha1 to ΔF508-CFTR did not change significantly when CAL is silenced. In sharp contrast, the binding Hsp90 is indeed increased subsequent to CAL silencing. HSP90 is viewed as a pro-folding decision point in the CFTR trafficking pathway. Thus, the improved CFTR-Hsp90 interactions would enhance the pro-folding pathway, improving ER to Golgi transport and diminishing ER arrest of ΔF508 CFTR. Our conclusion is further supported by the decrease we observed in the binding of ΔF508 CFTR to VCP. Taken together our results reveal that CAL knockdown leads to suppression of the anti-folding pathway for ΔF508 CFTR.

Results for NHERF1 further tie together the results of this study. NHERF1, a PDZ domain containing protein, anchors CFTR to the cytoskeleton through a protein complex involving ezrin [19]. Interaction between NHERF1 and ezrin is promoted by Rac1 activation, triggering a conformational change in NHERF1 that allows it to bind and stabilize ΔF508 CFTR [19]. Our data show that when CAL is inhibited by siRNA, there is an increase in NHERF1 in total lysate. These results suggest that steady state levels of NHERF1 increase when CAL is inhibited which then can anchor ΔF508 CFTR to the plasma membrane. We speculate that the reciprocal regulation of CAL and NHERF1 protein levels may reflect a cellular process which would ultimately determine the magnitude of CAL-dependent vs NHERF1-dependent trafficking to and residence at the plasma membrane. Overall, these results indicate that scaffold and chaperone protein levels will adjust intracellularly to support protein trafficking pathways with varying outcomes.

CAL interacts with other PDZ domain proteins such as the somatostatin subtype 5 and β1-adrenergic receptors [30]. In these PDZ domain containing proteins CAL functions in Golgi related processes. Although not studied, it is likely that given the results here, that CAL also plays a role in ER trafficking of these proteins. We speculate that CAL is located in the cytoplasm when it binds to the PDZ domain of ΔF508-CFTR and other relevant PDZ domain containing proteins. Such binding might play a role in maintaining ER morphology. Thus, alterations in CAL expression could affect the movement of ΔF508-CFTR and other relevant PDZ containing proteins out of the ER by altering its morphology. Alternately, CAL through its coiled-coil domain, might alter the trafficking of relevant PDZ containing proteins by direct interaction with another coiled-coil domain containing protein which is tethered to the ER via a transmembrane domain.

Our results provide a useful method for attaining cell surface expression of mature functional ΔF508 CFTR, by inhibiting CAL and thus blocking the interaction between CAL and CFTR. Discovering new ways to establish and enhance ΔF508 CFTR at the plasma membrane will provide more options for novel therapies.

Abbreviations

Aha1/AHSA1 (Activator of 90 kDa heat shock protein ATPase homolog 1); CAL (CFTR-Associated Ligand); NHERF1 (Na^+/H^+ Exchanger Regulatory Factor); PDZ (PSD-95, Dig, and ZO1); VCP (Valosin-containing protein).

Acknowledgements

We, the authors, thank Dr. Carolyn Machamer for the KDEL-td-tomato plasmid. We acknowledge Dr. Rajini Rao, Dr. Mark Donowitz, Dr. Carolyn Machamer, and Dr. J. Marie Hardwick for helpful discussions. We also thank Dr. Julia Romano for guidance regarding immunofluorescence and microscopy. This work was supported by NIH NHLBI grant #1F31HL128116 – 01 to EASB. The research was funding by the Cystic Fibrosis Foundation and an NHLBI multi-PI grant, R01 HL122267, to LC and WBG. We thank Kathryn A. Carson ScM Senior Research Associate for her support for statistical consulting. The latter was made possible by the Johns Hopkins Institute for Clinical and Translational Research which is funded in part by Grant Number 1UL1TR001079 from the National Center for Advancing Translational Sciences of the National Institutes of Health.

Disclosure Statement

The authors declare that WBG has a consultant agreement with the Vertex Corporation. LC has a license agreement with the Vertex Corporation for mutant cell lines. LC has a contract with Acetylon Pharmaceuticals. None of the authors have any financial interests that pertain directly to this work.

References

1 Kerem BS, Rommens JM, Buchanan JA, Markiewicz D, Cox TK, Chakravarti A, Buckwald M, Tsui LC: Identification of the cystic fibrosis gene: Genetic analysis. Sci 1989;245:1073-1080.
2 Pilewski JM, Frizzell RA: Role of CFTR in airway disease. Physiol Rev 1999;79:S215-S255.
3 Rosenstein BJ: Cystic fibrosis diagnosis: New dilemmas for an old disorder. Ped Pulm 2002;33:83-84.
4 Sheppard DN, Welsh MJ: Structure and function of the CFTR chloride channel. Physiol Rev 1999;79:S23-S45.
5 Sosnay PR, Siklosi KR, Van GF, Kaniecki K, Yu H, Sharma N, Ramalho AS, Amaral MD, Dorfman R, Zielenski J, Masica DL, Karchin R, Millen L, Thomas PJ, Patrinos GP, Corey M, Lewis MH, Rommens JM, Castellani C, Penland CM, Cutting GR: Defining the disease liability of variants in the cystic fibrosis transmembrane conductance regulator gene. Nat Genet 2013;45:1160-1167.
6 Sosnay PR, Castellani C, Corey M, Dorfman R, Zielenski J, Karchin R, Penland CM, Cutting GR: Evaluation of the disease liability of CFTR variants. Methods Mol Biol 2011;742:355-372.
7 Harrington MA, Gunderson KL, Kopito RR: Redox reagents and divalent cations alter the kinetics of cystic fibrosis transmembrane conductance regulator channel gating. J Biol Chem 1999;274:27536-27544.
8 Benharouga M, Sharma M, Lukacs GL: CFTR folding and maturation in cells. Methods Mol Med 2002;70:229-243.
9 Cheng J, Moyer BD, Milewski M, Loffing J, Ikeda M, Mickle JE, Cutting GR, Li M, Stanton BA, Guggino WB: A Golgi-associated PDZ domain protein modulates cystic fibrosis transmembrane regulator plasma membrane expression. J Biol Chem 2002;277:3520-3529.
10 Neudauer CL, Joberty G, Macara IG: PIST: a novel PDZ/coiled-coil domain binding partner for the rho-family GTPase TC10. Biochem Biophys Res Comm 2001;280:541-547.
11 Cheng J, Wang H, Guggino WB: Modulation of mature cystic fibrosis transmembrane regulator protein by the PDZ domain protein CAL. J Biol Chem 2004;279:1892-1898.
12 Cheng J, Wang H, Guggino WB: Regulation of cystic fibrosis transmembrane regulator trafficking and protein expression by a Rho family small GTPase TC10. J Biol Chem 2005;280:3731-3739.
13 Cheng J, Cebotaru V, Cebotaru L, Guggino WB: Syntaxin 6 and CAL mediate the degradation of the cystic fibrosis transmembrane conductance regulator. Mol Biol Cell 2010;21:1178-1187.
14 Lee HW, Cheng J, Kovbasnjuk O, Donowitz M, Guggino WB: Insulin-like growth factor 1 (IGF-1) enhances the protein expression of CFTR. PLoS One 2013;8:e59992.

15 Wolde M, Fellows A, Cheng J, Kivenson A, Coutermarsh B, Talebian L, Karlson K, Piserchio A, Mierke DF, Stanton BA, Guggino WB, Madden DR: Targeting CAL as a negative regulator of DeltaF508-CFTR cell-surface expression: an RNA interference and structure-based mutagenetic approach. J Biol Chem 2007;282:8099-8109.
16 Cheng SH, Gregory RJ, Marshall J, Paul S, Souza DW, White GA, O'Riordan CR, Smith AE: Defective intracellular transport and processing of CFTR is the molecular basis of most of cystic fibrosis. Cell 1990;63:827-834.
17 Lukacs GL, Chang XB, Bear C, Kartner N, Mohamed A, Riordan JR, Grinstein S: The delta F508 mutation decreases the stability of cystic fibrosis transmembrane conductance regulator in the plasma membrane. Determination of functional half-lives on transfected cells. J Biol Chem 1993;268:21592-21598.
18 Gee HY, Noh SH, Tang BL, Kim KH, Lee MG: Rescue of DeltaF508-CFTR trafficking via a GRASP-dependent unconventional secretion pathway. Cell 2011;146:746-760.
19 Loureiro CA, Matos AM, Dias-Alves A, Pereira JF, Uliyakina I, Barros P, Amaral MD, Matos P: A molecular switch in the scaffold NHERF1 enables misfolded CFTR to evade the peripheral quality control checkpoint. Sci Signal 2015;8:ra48.
20 Schneider EK, Reyes-Ortega F, Li J, Velkov T: Can cystic fibrosis patients finally catch a breath with Orkambi? Clin Pharm Ther 2016;101:130-141.
21 Goldstein RF, Niraj A, Sanderson TP, Wilson LS, Rab A, Kim H, Bebok Z, Collawn JF: VCP/p97 AAA-ATPase does not interact with the endogenous wild-type cystic fibrosis transmembrane conductance regulator. Amer J Resp Cell Molec Biol 2007;36:706-714.
22 Wang X, Matteson J, An Y, Moyer B, Yoo JS, Bannykh S, Wilson IA, Riordan JR, Balch WE: COPII-dependent export of cystic fibrosis transmembrane conductance regulator from the ER uses a di-acidic exit code. J Cell Biol 2004;167:65-74.
23 Vij N, Fang S, Zeitlin PL: Selective inhibition of endoplasmic reticulum-associated degradation rescues DeltaF508-cystic fibrosis transmembrane regulator and suppresses interleukin-8 levels: therapeutic implications. J Biol Chem 2006;281:17369-17378.
24 Younger JM, Ren HY, Chen L, Fan CY, Fields A, Patterson C, Cyr DM: A foldable CFTR{Delta}F508 biogenic intermediate accumulates upon inhibition of the Hsc70-CHIP E3 ubiquitin ligase. J Cell Biol 2004;167:1075-1085.
25 Choo-Kang LR, Zeitlin PL: Induction of HSP70 promotes DeltaF508 CFTR trafficking. Amer J Physiol Lung Cell Mol Physiol 2001;281:L58-L68.
26 Farinha CM, Nogueira P, Mendes F, Penque D, Amaral MD: The human DnaJ homologue (Hdj)-1/heat-shock protein (Hsp) 40 co-chaperone is required for the *in vivo* stabilization of the cystic fibrosis transmembrane conductance regulator by Hsp70. Biochem J 2002;366:797-806.
27 Wang X, Venable J, LaPointe P, Hutt DM, Koulov AV, Coppinger J, Gurkan C, Kellner W, Matteson J, Plutner H, Riordan JR, Kelly JW, Yates JR, III, Balch WE: Hsp90 cochaperone Aha1 downregulation rescues misfolding of CFTR in cystic fibrosis. Cell 2006;127:803-815.
28 Koulov AV, LaPointe P, Lu B, Razvi A, Coppinger J, Dong MQ, Matteson J, Laister R, Arrowsmith C, Yates JR, III, Balch WE: Biological and structural basis for Aha1 regulation of Hsp90 ATPase activity in maintaining proteostasis in the human disease cystic fibrosis. Mol Biol Cell 2010;21:871-884.
29 Skach WR: CFTR: new members join the fold. Cell 2006;127:673-675.
30 Guggino WB, Stanton BA: New insights into cystic fibrosis: molecular switches that regulate CFTR. Nat Rev Mol Cell Biol 2006;7:426-436.